The Holomorphic Embedding Loadflow Method for DC Power Systems and Nonlinear DC Circuits

Antonio Trias and José Luis Marín

***Abstract*—The Holomorphic Embedding Loadflow Method is extended here from AC to DC-based systems. Through an appropriate embedding technique, the method is shown to extend naturally to DC power transmission systems, preserving all the constructive and deterministic properties that allow it to obtain the white branch solution in an unequivocal way. Its applications extend to nascent meshed HVDC networks and also to power distribution systems in more-electric vehicles, ships, aircraft, and spacecraft. In these latter areas, it is shown how the method can cleanly accommodate the higher-order nonlinearities that characterize the I-V curves of many devices. The case of a photovoltaic array feeding a constant-power load is given as an example. The extension to the general problem of finding DC operating points in electronics is also discussed, and exemplified on the diode model.**

***Index Terms*—Circuit analysis computing, load flow, nonlinear network analysis, power system analysis computing, power system modeling, power system simulation, space technology.**

I. Introduction

THE Holomorphic Embedding Loadflow Method (HELM) is both a novel technique for solving and a theoretical framework for analyzing the AC powerflow problem [1], [2]. It is based on a complex-valued embedding technique specifically devised to exploit the particular algebraic nonlinearities of the powerflow problem. This is in contrast with powerflow methods that use numerical iteration, which is a generic root-finding technique that applies to any type of nonlinearity. HELM's distinct advantages stem from its direct and constructive nature: the method unequivocally arrives to the selected operational solution if it exists, and conversely it unequivocally signals unfeasibility when such solution does not exist. Additionally, its underlying theoretical framework, based on the algebraic geometry of plane algebraic curves, is a source of new insights and analytical tools for this old problem [3].

Powerflow studies are widely used in utility AC grids (see [4] for a review), but the problem is less commonly known under that name in DC systems. Part of the reason is that utility-size meshed HVDC systems are still at their early stage of development [5]. Another reason is that practitioners of DC power electronics do not refer to this problem by the same name, instead using the generic term "nonlinear analysis" of the steady state [6], [7] (also referred to as operating point, or bias point). In any case, the mathematical problem in DC is very similar to its counterpart in AC, and it would be completely analogous if the only nonlinear devices present in the circuit were constant power loads.

In the context of onboard DC power distribution systems in spacecraft and in so-called "more-electric" aircraft, ships, and vehicles, the power network is commonly referred to as the Power Management and Distribution (PMAD) system [8]. In modern PMAD systems, constant power loads play a major role. These are mainly DC motors, as well as other tightly regulated loads. Constant power loads also play important roles in smaller DC power electronic systems, such as computers. In all these cases, the powerflow analysis is performed in the guise of the standard nonlinear analysis for finding the DC operating point (or points) of the circuit. Classical tools, such as the well-known program SPICE used in analog electronics design, contain algorithms for this calculation [9].

Just like their counterparts in AC systems [10]–[12], powerflow algorithms for DC systems have all one thing in common, which is their reliance on *numerical iteration* as the root-finding technique lying at the core of the procedure. Examples of these are Gauss-Seidel iteration and the widely used Newton-Raphson method, in its many variants. Some powerflow algorithms improve on the performance and convergence properties of these core iterative methods by using homotopy (continuation methods) [13]–[15]. Other algorithms utilize alternative techniques such as evolutionary algorithms [16] or interval arithmetic [17], with the aim of improving global convergence. However, they all use Newton-Raphson or similar contraction map iterations to zero-in on the solutions. In this regard, DC iterative methods suffer from the problem of dependence on the choice of the initial point just as much as their AC counterparts, and this dependence can become highly sensitive in some regions [18]–[22].

This paper extends HELM to DC systems, preserving the constructive and deterministic properties that allow it to obtain the desired solution in an unequivocal way. It also goes one step further by contemplating nonlinear devices other than constant power loads, which are more commonly found in DC. But it should be remarked that the benefits derived from DC HELM are not only reliable calculations. It has been found that the simpler treatment allowed by DC systems is conductive to richer theoretical results, which in turn bring more insights and new results (some of which revert back to AC systems as well).

The rest of the paper is structured as follows: in Section II, HELM is adapted to DC power systems with linear components

Manuscript received August 6, 2015; revised November 22, 2015; accepted December 8, 2015. This paper was recommended by Associate Editor J. M. Olm.

A. Trias is with Aplicaciones en Informatica Avanzada, 08172 Barcelona, Spain (e-mail: triast@aia.es).

J. L. Marín is with Gridquant, 08172 Barcelona, Spain (e-mail: marinjl@gridquant.com).

Color versions of one or more of the figures in this paper are available online at http://ieeexplore.ieee.org.

Digital Object Identifier 10.1109/TCSI.2015.2512723

and constant power loads. Section III then extends the method to power systems including devices with nonlinearities of a more general nature. Section IV presents a model of a photovoltaic panel feeding a constant power load, as an example of a power system containing higher order nonlinearities. Section V presents an example of a general (non-power) DC circuit, a simple diode, which shows how the HELM methodology can be extended to a problem that is far removed from the field of power transmission, in which the method originated. Section VI is dedicated to a discussion comparing HELM methods to other state of the art iterative methods, dwelling on the conceptual differences, advantages and disadvantages, and showing some results. The Appendix shows how to best calculate Padé approximants in the context of the method, including a discussion on how to avoid numerical stability and precision issues.

II. Adapting HELM to DC Systems

Consider a general DC power network consisting of linear devices and constant power loads. Constant power generation, although less common, is also contemplated by allowing loads of opposite sign. The power flow equations that describe the steady state of such system, written in terms of the current balance at each bus, are

$$\sum_j G_{ij}^{(\mathrm{tr})} V_j + G_i^{(\mathrm{sh})} V_i = -\frac{P_i}{V_i} \tag{1}$$

where the summation runs over all buses j, including swing buses (at least one swing is assumed). The index i varies over all unknown variables V_i, that is, there is one equation for each non-swing bus i. Here $G_{ij}^{(\mathrm{tr})}$ is the transmission conductance matrix, $G_i^{(\mathrm{sh})}$ represents shunt conductances and resistive loads, and P_i is a constant power load. Contrary to the convention in AC power flow, the so-called passive sign convention is adopted here, i.e., P_i is positive for loads and negative for generators.

The key to extend HELM to this problem lies in two of the fundamental driving ideas presented in [2]: exploiting the specific algebraic structure of the problem, and doing so guided by the particular *projective invariance* of (1). Embedding techniques, as a general concept, exploit the smoothness of the functions involved, as it is done for instance in homotopic continuation methods. But the evidently simple algebraic structure of powerflow equations suggests that one could do much better if the embedding could preserve *holomorphicity*, which is a much stronger condition (see the detailed discussion in Section VI on the comparison with continuation methods). On the other hand, the projective invariance of the equations links the global scale of voltages (or equivalently, the choice of swing voltage) with a global scaling of constant-power injections: if one makes the change of variables $V_k' \equiv \lambda V_k$, the equations recover exactly the same form after rescaling the injections as $P_i' \equiv \lambda^2 P_i$. This naturally suggests an embedding that scales constant-power injections, which has the additional appeal of mimicking the physics of an energized transmission network as it gets loaded gradually and uniformly. The end result is an embedding that ensures holomorphicity and, moreover, effectively converts the powerflow problem into a study of (complex) *algebraic curves*.

In contrast with the AC case, all magnitudes involved here are now real instead of complex, but it is essential that the embedding parameter is complex because it is only by working in the complex plane that the whole structure of solution branches can be found. Among other reasons, this is a consequence of the fundamental theorem of algebra, which ensures that the algebraic curve, being a polynomial, always has n roots, n being the degree of the polynomial. Additionally, working in the complex plane guarantees the application of Stahl's theorem [23], [24], which is essential for the convergence and maximality of the analytic continuation procedure used in the numerical summation of the power series.

The proposed embedding is then as follows:

$$\sum_j G_{ij}^{(\mathrm{tr})} V_j(s) = -s G_i^{(\mathrm{sh})} V_i(s) - \frac{s P_i}{V_i(s)} \tag{2}$$

where s is a complex parameter. Constant power loads and shunt-connected devices are embedded directly in s, so that they all vanish at $s = 0$. The aim is to obtain a reference state at $s = 0$ that represents a linear, pure transmission network energized by the swing bus, but having no connected loads. Embedding shunt terms is not essential, but it simplifies the reference state and moreover it mirrors closer what actually takes place when progressively loading a network.

Multiplying equations (2) by V_i to eliminate denominators makes it explicit that they are polynomial, and therefore define the voltages $V_i(s)$ as space algebraic curves. Standard elimination procedures (such as, among others, Buchberger's algorithm [25] for finding a Gröbner basis of the system) allow one to arrive to a single polynomial equation in one of the unknowns, while the rest are eliminated in a triangular fashion. Such elimination polynomial is expensive to compute explicitly in networks larger than just a few buses, but the important point is that the embedded system (2) is thus proven to be an algebraic curve. Notice that in contrast to the AC problem, where one has to take special care to get rid of the complex conjugation operation by introducing additional variables $\widehat{V}_i(s)$, here there is no need to do so. The equivalent counterpart of the reflection condition is simply

$$V_i(s) = V_i^*(s^*) \tag{3}$$

which is a requirement for solutions to be real for s real. Solutions that do not satisfy (3) are "ghost" solutions, i.e., they are not physically realizable.

Next, standard techniques for manipulating formal power series [26] are used to numerically compute solutions. The main goal is to obtain the operational solution, but let us initially consider the power series expansion (about the point $s = 0$) of any of the multiple branches, i.e., any of the so-called *germs* of the multi-valued holomorphic function $V_i(s)$ defined by the algebraic curve

$$V_i(s) = \sum_n^{\infty} V_i[n] s^n.$$

The function $1/V_i(s)$ appearing on the right hand side in (2) also has a power series expansion $1/V_i(s) = \sum_n^{\infty} V_i^{-1}[n]\ s^n$,

whose coefficients are related to those of $V_i(s)$ by the following expressions:

$$V_i[0]V_i^{-1}[0] = 1$$
$$\sum_{k=0}^{n} V_i[k]V_i^{-1}[n-k] = 0 \qquad (n \geq 1) \tag{4}$$

This can be deduced from the power series of the constant function $1 = V(s) \cdot 1/V(s)$. Plugging the expressions for these power series into equations (2) and extracting the coefficients at an arbitrary order in s, say $N+1$, the following linear system is obtained:

$$\sum_j G_{ij}^{(\mathrm{tr})} V_j[N+1] = -G_i^{(\mathrm{sh})} V_i[N] - P_i V_i^{-1}[N]. \tag{5}$$

The left hand side contains the unknowns (the coefficients at order $N+1$), while everything else on the right hand side is composed of coefficients at order N or lower. By starting recurrence relation (5) at order zero with an adequate choice of germ, the progressive solution in sequence of these systems provides the construction of the power series up to any desired order. This involves of course the calculation of the coefficients appearing on the right hand side, which are obtained in this case through the use of relations (4). It is important to remark that the conductance matrix $G_{ij}^{(\mathrm{tr})}$ remains fixed; therefore its factorization needs to be performed only once.

The choice of a reference germ with which to bootstrap the calculations in (5) is of key importance. After all, this choice determines which solution branch will be propagated by analytical continuation in the final part of the procedure. In fact, the embedding has been devised so that making this choice at $s = 0$ is both possible and straightforward. When $s = 0$, the embedded system has only one possible solution satisfying $V_i(0) \neq 0$ at all buses. Moreover, this solution makes physical sense as an energized but unloaded transmission network (i.e., $V_i[0] = V_{\mathrm{sw}}$, the swing source, for all i). The branch generated by this germ is therefore labeled as the "white" branch. At the $s = 0$ limit, all other power flow solutions, whether physical or not, contain one or more buses whose voltage is zero; such germs would generate "black" branches and "ghost" (unphysical) branches.

The method concludes with the numerical evaluation of the germ at the desired point $s = 1$ by means of analytic continuation techniques. In particular, the method prescribes Padé approximants [27] because, by Stahl's theorem [23], [24] the sequences of near-diagonal Padé approximants converge to the actual function in its maximal domain of analytical continuation (in the capacity sense). In practice, the "stairstep" sequence along the diagonal and superdiagonal of the Padé table, which is equivalent to the convergents of the continued fraction of the power series, is the most efficient one. Thanks to Stahl's result, if the solution on this branch exists at $s = 1$, then it will be found because the Padé approximants converge; and conversely, if it does not exist then the Padé approximants will not converge.

In addition to providing a direct numerical method for computing solutions, HELM provides a rigorous grounding for the problem of identifying the operational solution in power systems, as argued in [1], [2]. As some authors have demonstrated, criteria based exclusively on the stability of the solution are not sufficient to unambiguously select which is the operational solution [28]. HELM's *proposal* is that the operational solution is defined as the one that continuously connects, in the analytic continuation sense, to the well-defined reference state at $s = 0$ described above. Note that this is an argument based on physics and continuity, not on mathematics. While it is certainly possible for a power system to enter into an operating state that is not the white branch proposed by HELM, the physics of power systems shows that such states are sub-optimal (i.e., they have greater line losses) [29].

III. Devices With Higher-Order Nonlinearities

In many DC power systems of interest it is common to find nonlinear devices other than constant power loads. This is certainly the case in power electronics, where one finds I-V characteristic curves of many different types. In the following, it is shown how to accommodate these in the HELM framework.

For the purposes of this discussion, nonlinearities are divided into two broad categories: those arising from sharp changes of regime (e.g., saturation effects, limits, sharp steps, etc.) vs. those that are smooth (i.e., differentiable). Nonlinearities of the former type have to be treated out of HELM methodology properly speaking, since they are not conductive to a holomorphic treatment.[1] In this paper it is assumed that the method is applied piecewise on each smooth regime, leaving the global problem of non-smoothness for future work.

Let us consider a DC network containing nonlinear devices:

$$\sum_j G_{ij}^{(\mathrm{tr})} V_j + G_i^{(\mathrm{sh})} V_i + \sum_j I_{ij}^{(\mathrm{tr})}(V_j, V_i) + I_i^{(\mathrm{sh})}(V_i) = -\frac{P_i}{V_i}. \tag{6}$$

The second summation on the left hand side runs over the series-connected nonlinear devices at bus i, which are assumed to have I-V characteristics given by the functions $I_{ij}^{(\mathrm{tr})}(V_j, V_i)$. Each bus i may also have shunt-connected nonlinear devices, having an I-V characteristic given by $I_i^{(\mathrm{sh})}(V_i)$.

Now if this system were representing a general nonlinear electronic circuit, then there would not be a clear *a priori* guide as to how to embed it, because such systems have in general several possible DC operating points (sometimes purposefully by design). But if, on the other hand, the network has been designed for *power transmission and delivery*, then it is plausible to postulate that the desired DC operating point can be defined as it was done for AC power systems: a state that connects back (in the analytic continuation sense) to an energized network with no loads or injections. With this guidance, the proposed embedding is as follows:

$$\sum_j G_{ij}^{(\mathrm{tr})} V_j = (s-1) \sum_j G_{ij}^{(\mathrm{nl})} V_j - s \sum_j I_{ij}^{(\mathrm{tr})}(V_j, V_i) - s I_i^{(\mathrm{sh})}(V_i) - s G_i^{(\mathrm{sh})} V_i - \frac{s P_i}{V_i}. \tag{7}$$

[1] In principle, the method could still apply after these have been approximated by smooth functions, but the authors have not explored this possibility yet.

Series-connected nonlinear devices are embedded in such a way that their effect at $s = 0$ is equivalent to a resistive transmission link, thus contributing a conductance matrix entry $G_{ij}^{(\mathrm{nl})}$. This is done so that the analytic continuation of the reference state at $s = 0$ can be *a priori* connected with the operational solution at $s = 1$, when all loads and devices are connected (otherwise some nodes would be isolated at $s = 0$). The suggested value to use for $G_{ij}^{(\mathrm{nl})}$ is the corresponding ratio $I(V)/V$ obtained at the nominal operating voltage of the power network. By contrast, constant power loads and shunt-connected devices are all embedded directly in s as before, so that they vanish at $s = 0$. Thus the reference state at $s = 0$ is given by a linear, pure transmission network energized by the swing bus, but having no connected loads.

Considering the power series expansions of the voltages and the nonlinear I-V functions involved in (7), the relation for the coefficients at order $N + 1$ is:

$$\sum_j \left(G_{ij}^{(\mathrm{tr})} + G_{ij}^{(\mathrm{nl})}\right) V_j[N+1] = \sum_j G_{ij}^{(\mathrm{nl})} V_j[N] - \sum_j I_{ij}^{(\mathrm{tr})}[N] - I_i^{(\mathrm{sh})}[N] - G_i^{(\mathrm{sh})} V_i[N] - P_i V_i^{-1}[N]. \quad (8)$$

The left hand side of this system contains the unknowns, and everything else on the right hand side depends on coefficients at order N or lower. Just like $V_i^{-1}[N]$ in relation (4), it is found that the coefficients $I_{ij}^{(\mathrm{tr})}[N]$ and $I_i^{(\mathrm{sh})}[N]$ can also be obtained as a function of the coefficients of the voltage, $V_i[0], \ldots, V_i[N]$. The examples in Sections IV and V show how to obtain such relations for non-trivial nonlinear functions. The rest of the procedure would be the same as in Section II.

It should be emphasized that the embedding proposed in (7) is only a reasonable one, *a priori*, for this generic power system. Depending on the specific nature of the nonlinearities involved, a different embedding may be found more adequate, but the guiding principles would be the same. The next section provides an example.

IV. Photovoltaic Panel Feeding a Constant Power Load

Let us consider a simplified model consisting of one solar photovoltaic (PV) panel source coupled to a DC-DC buck converter feeding a load tightly regulated to have a constant-power characteristic. Some authors have proposed this as a simplified model of the relevant behavior of DC power distribution systems aboard spacecraft [30], [31]. Fig. 1 displays a schematic view of this system. The solar PV panel has a characteristic I-V curve with high nonlinearity. It is commonly approximated by a high order polynomial

$$I(V_1) = I_{\mathrm{SC}} \left(1 - \left(\frac{V_1}{V_{\mathrm{OC}}}\right)^K\right) \quad (9)$$

where I_{SC} is the short circuit current and V_{OC} is the open circuit voltage of the panel. A value of $K = 33$ provides accuracy within 2% of experimental results [31]. The panel output is fed to the converter through a distribution line with resistance R_{12}.

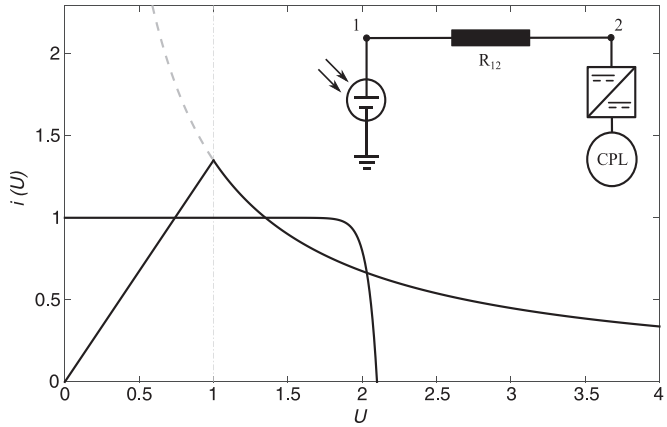

Fig. 1. Solar panel feeding a DC-DC converter coupled to a constant power load.

The effective I-V characteristic of the converter plus regulated load system shows two very different regimes depending on the value of its input voltage, one being constant-power and the other one being linear resistive

$$I(V_2) = \begin{cases} \frac{V_{\mathrm{reg}}^2}{R_L V_2} & \text{if } V_2 > V_{\mathrm{reg}} \\ \frac{V_2}{R_L} & \text{if } V_2 \le V_{\mathrm{reg}} \end{cases} \quad (10)$$

In the following, the holomorphic embedding method will only be applied to the desirable regime, $V_2 > V_{\mathrm{reg}}$, where the regulation can sustain a constant power draw. Of course the results would have to be checked after the fact, to verify that V_2 is indeed within this regime. The equations of the system are thus

$$I_{\mathrm{SC}} \left(1 - \left(\frac{V_1}{V_{\mathrm{OC}}}\right)^K\right) = \frac{V_1 - V_2}{R_{12}}$$

$$\frac{V_1 - V_2}{R_{12}} = \frac{V_{\mathrm{reg}}^2}{R_L V_2}$$

For the purpose of exemplifying how to deal with higher order nonlinearities, the system will be approximated by making the resistance of the transmission line $R_{12} = 0$, which is a reasonable assumption in real systems and does not change the essence of the following derivation. Then $V_1 = V_2 \equiv V$, and the system reduces to a single equation

$$I_{\mathrm{SC}} \left(1 - \left(\frac{V}{V_{\mathrm{OC}}}\right)^K\right) = \frac{V_{\mathrm{reg}}^2}{R_L V}.$$

The notation is simplified by working with the dimensionless magnitudes $U \equiv V/V_{\mathrm{reg}}$, $U_0 \equiv V_{\mathrm{OC}}/V_{\mathrm{reg}}$, and $p \equiv V_{\mathrm{reg}}/(I_{\mathrm{SC}} R_L)$

$$1 - \left(\frac{U}{U_0}\right)^K = \frac{p}{U}. \quad (11)$$

Disregarding the undesired regime defined by (10), it is straightforward to verify graphically that this system may have two, one, or zero solutions. A single solution is obtained at the

tangency limit, which can be obtained as the point where (11) and its derivative have a common zero

$$U^{\mathrm{crit}} = p\left(1+\frac{1}{K}\right)$$
$$U_0^{\mathrm{crit}} = \frac{(1+K)^{1+\frac{1}{K}}}{K}p. \tag{12}$$

Notice that U_0^{crit} is proportional to p, and the proportionality constant only depends on K. For $U_0 > U_0^{\mathrm{crit}}$ the system has two solutions, while for $U_0 < U_0^{\mathrm{crit}}$ it has none. This of course assumes that the system is operating in the desired regime, i.e., $1 < U < U_0$ in this case.

A. Holomorphic Embedding. White Branch

The physics of this circuit naturally suggests a holomorphic embedding completely analogous to the one used in general AC power systems

$$1-\left(\frac{U(s)}{U_0}\right)^K = \frac{sp}{U(s)} \tag{13}$$

where the reference solution at $s=0$ is clearly realizable (open circuit state) and can be physically continued to the solution in the branch with higher voltage. For the purpose of labeling, this will be referred to as the "white" branch.

To put this into correspondence with the general treatment given in (7), note that the PV panel, i.e., the left hand side in (13), plays the role of an injection $I_i^{(\mathrm{sh})}(V_i)$, *not* a series device. However, in this simple example it has not been embedded under s because it is the only energy source.

Using the power series expansion of $U(s)$ about $s=0$, plus the corresponding one for the function $1/U(s)$, and plugging them into (13), one would obtain, after extracting the terms at a given order N on both sides of the equation, a relationship for the coefficients of $U(s)$. To make this relationship explicit, a useful technique will be used, which is of general applicability when working with power series. It exploits the fact that the coefficients of a power series and those of its derivative are related to each other in a very simple way. Defining the auxiliary function $R(s) \equiv (U(s)/U_0)^K$ and taking the logarithmic derivative with respect to s on both sides of it, one obtains:

$$U(s)R'(s) = KR(s)U'(s).$$

Using the power series expansion of both $U(s)$ and $R(s)$, and plugging them into this equation, one obtains the following relation for the coefficients at order N:

$$R[N+1]U[0] + \sum_{k=0}^{N-1}\left(\frac{k+1}{N+1}\right)R[k+1]U[N-k]$$
$$= KU[N+1]R[0] + K\sum_{k=0}^{N-1}\left(\frac{k+1}{N+1}\right)U[k+1]R[N-k] \tag{14}$$

where the highest order terms have been singled out. Note that from (13) the term $R[N+1] = -pU^{-1}[N]$. Therefore relation (14) provides $U[N+1]$ from terms that are all known from the preceding orders. At this point, the choice of germ is introduced: the reference solution here is such that $U(0) = U_0$, and thus $U[0] = U_0$ and $R[0] = 1$. This provides the values to start the recurrence relation and thus the method constructs the "white germ." The rest of the procedure consists in performing the analytic continuation of the power series of the voltages, using Padé approximants as prescribed by the method.

B. Black Branch

In this case the other solution can also be calculated by an analogous procedure. Intuitively, this branch is such that $U \to 0$ as $s \to 0$, but approaching a finite current in the power flow equation (short circuit condition). Therefore it is reasonable to tentatively represent the voltage explicitly as $U(s) = sX(s)$, so that the equation becomes

$$1 - s^K\left(\frac{X(s)}{U_0}\right)^K = \frac{p}{X(s)}.$$

This indeed admits a unique solution at $s=0$ such that $X(0) \neq 0$, namely $X(0) = p$. This is key, as it provides the selection of the desired germ for the constructive procedure that follows. The branch generated by this germ will be referred to as "black."

One technical difficulty should be addressed first. Notice how the s variable only appears in this equation as the power s^K. Under the s-representation, the power series for $X(s)$ would be lacunary, i.e., it would have many gaps in its terms since all of them would be powers that are multiple of K. For large K this would generate numerical problems, in general. But thanks to holomorphicity, this problem can be completely avoided, simply using the variable $t \equiv s^K$:

$$1 - t\left(\frac{X(t)}{U_0}\right)^K = \frac{p}{X(t)}. \tag{15}$$

This can be viewed as a *reparameterization* of the underlying algebraic curve. Similarly to the previous case, defining an auxiliary function $T(t) \equiv (X(t)/U_0)K$ and taking the logarithmic derivative with respect to t on both sides of this definition, one obtains a relation completely analogous to (14) in the former case:

$$T[N+1]X[0] + \sum_{k=0}^{N-1}\left(\frac{k+1}{N+1}\right)T[k+1]X[N-k]$$
$$= KX[N+1]T[0] + K\sum_{k=0}^{N-1}\left(\frac{k+1}{N+1}\right)X[k+1]T[N-k] \tag{16}$$

The reparameterized powerflow (15) yields a slightly different relationship this time:

$$T[N] = -pX^{-1}[N+1]. \tag{17}$$

These last two relations are sufficient to construct the power series for $X(s)$. In this case the black branch germ is such that $X[0] = p$ and therefore $T[0] = (p/U_0)^K$. With these starting values, one would first use (17) and the relation for the reciprocal series (4) to obtain $X[N+1]$, and then use (16)

TABLE I
NUMERICAL RESULTS APPROACHING THE CRITICAL TANGENCY POINT

δp	U_{white}	N_{white}	U_{black}	N_{black}
0.1	1.877456	39	1.647165	9
0.01	1.827381	214	1.760707	19
0.001	1.807456	684	1.786533	54
0.0001	1.801180	924	1.793967	259
0.00001	1.800051	1024	1.796230	939
0.000001	1.799541	1679	1.796659	619

to obtain $T[N+1]$. Analogously, one would evaluate the resulting power series using (near diagonal) Padé approximant sequences. Stahl's theorem applies equally to this case, as it is simply a different power series germ of the same algebraic curve.

C. Operational vs. Non-Operational Branch

In the treatment above, the two branches were referred to as white and black, refraining from designating them as desired vs. undesired, or operational vs. non-operational (let alone stable vs. unstable). However, as the system under study is a power delivery network, it is evident that the white branch is the desired one for operation, as it delivers the same power using higher voltage and smaller current. In systems whose design goal is not power delivery, this designation needs to be assessed on each articular case (cf. next section). Therefore, when using HELM for general electric circuits, the method does not automatically select "the" operational solution; rather, the practitioner needs to make this choice herself by designing an adequate embedding and selecting the desired germ at the reference state. How to do this in general is still an open question.

D. Numerical Results

The ability of the method to constructively calculate both solution branches was tested by performing some numerical experiments. Table I shows the results obtained for each branch as the parameter p is varied towards the point of tangency p_{crit} given by (12), where the two solutions merge. The parameter U_0 was kept fixed at $U_0 = 2.0$ and the exponent at $K = 33$. Requiring a fixed error tolerance of 10^{-8}, the table shows the maximum order of the power series needed to achieve it, as a function of the distance $\delta p = p_{\text{crit}} - p$.

As shown on the table, the accuracy is remarkable, even when in very close proximity to the point of collapse. Additionally, it was found that even at very high orders of the Padé approximants the numerical results are still stable, with orders up to $N = 2000$ still possible within the limits of double-precision arithmetic. The numerical stability was found to be in general much better than in comparable AC systems, while the computational cost is of course smaller due to the use of real arithmetic.

For comparison, the same problem was solved using the classical Newton-Raphson (N-R) method. As expected, the results exhibit the dependence with respect to the initial seed, with fractality phenomena appearing on the bordering region between the two solutions. Fig. 2 shows these results by coloring the two solutions the iterations can converge to. The x-axis represents the initial value of voltage used as a seed for the iteration, while the y-axis represents different values of the dimensionless load parameter p. Points in green represent seeds that converge to the white branch, red ones those that converge to the black branch, and black ones those that have not converged after 50 iterations. A few points shown in yellow represent convergence to a wrong value, within the error tolerance used (10^{-6}). For all values of U_0 the situation is qualitatively the same, although the fractal region grows larger for higher values of U_0.

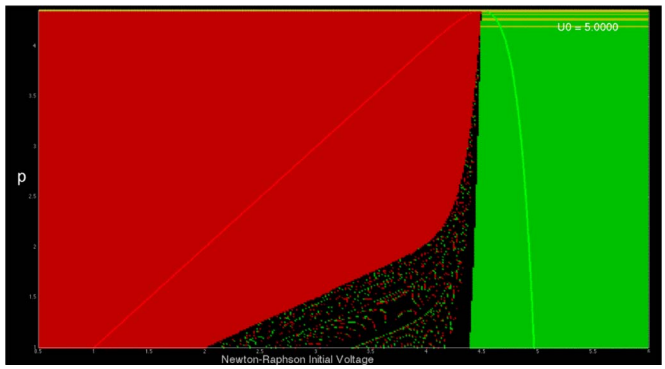

Fig. 2. Solutions obtained with the Newton-Raphson method, depending on the choice of the initial point. The lines in pale red and green mark the location of the actual "black" and "white" branches, respectively.

V. OPERATING POINT OF A DIODE CIRCUIT

This section exemplifies how the fundamental ideas behind HELM methodology can be applied to the general problem of finding the DC operating point(s) of nonlinear circuits, other than power systems. Two main differences arise here: one, how to make the proper choice for the holomorphic embedding, which is not as obvious, in general; the other, how to identify and select the desired reference solution at the point $s = 0$. These two issues are of course intimately linked, as the choice of embedding is normally guided by some intuition about what the reference solution should be. The previous sections have shown that power systems provide a clear physical intuition for this (see also the canonical embedding described in [2]), but for general DC circuits one must study each particular case. Although it is not possible to give a generic recipe, the driving idea is that one should strive to get a reasonable and realizable reference state, such that, *a priori*, it can be connected (in the analytic continuation sense) to the desired solution.

In order to show how this can be done, a simple diode circuit is analyzed. As shown in Fig. 3, a constant voltage source E feeds a diode through a line with resistance R_1, followed by a resistive load R_2. Disregarding the breakdown region for high reverse polarization, the ideal diode has an I-V characteristic given by the Shockley equation

$$I_{\text{D}}(V_{\text{D}}) = I_{\text{S}} \left(e^{\frac{V_{\text{D}}}{n V_T}} - 1 \right)$$

where V_T is the thermal voltage (approximately 26 mV at room temperatures) and I_{S} is the reverse bias saturation current (values typically in the μA range). The ideality factor n

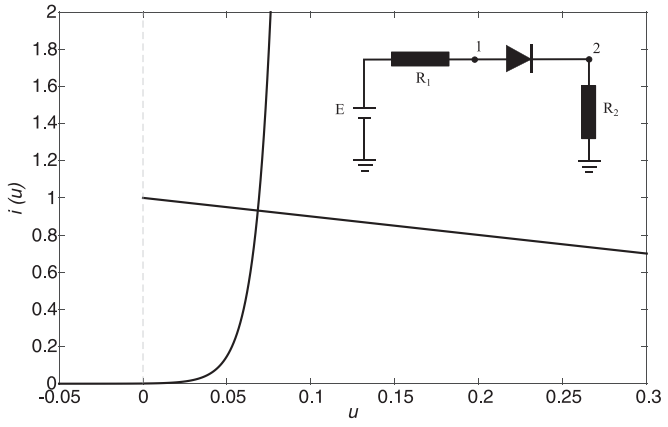

Fig. 3. Graphical solution of the diode circuit.

will be taken to be 1, without losing generality. The circuit equations are

$$\frac{E - V_1}{R_1} = I_{\mathrm{D}}(V_1 - V_2) = \frac{V_2}{R_2}. \tag{18}$$

Since a forward bias $E > 0$ is assumed, one has $0 < V_2 < V_1 < E$. Defining dimensionless quantities $U_1 \equiv V_1/E, U_2 \equiv V_2/E, u \equiv (V_1 - V_2)/E$, and eliminating U_1 from (18), one obtains

$$u = 1 - \left(1 + \frac{R_1}{R_2}\right) U_2.$$

Eliminating U_2 from (18), and defining the dimensionless constants $u_T \equiv V_T/E, \varepsilon \equiv (R_1 + R_2)I_{\mathrm{S}}/E$, one finally obtains:

$$\varepsilon \left(e^{\frac{u}{u_T}} - 1\right) = 1 - u. \tag{19}$$

It is easy to see graphically that this equation has a single positive solution in the interval (0,1), given by the intersection of $\varepsilon(e^{u/u_T} - 1)$ with the line $1 - u$ (see Fig. 3).

In Sections III and IV-C it was shown how networks designed for power transmission have a natural choice for the embedding and the reference state at $s = 0$. Here instead we are confronted with a general nonlinear DC system, for which there is no clear criterion to guide us. This is an open question and therefore the best that can be done is to study it on a case-by-case basis. In our case, looking at (19), the following holomorphic embedding is proposed:

$$\varepsilon \left(e^{\frac{u(s)}{u_T}} - 1\right) = 1 - su(s). \tag{20}$$

This has a well-defined reference state at $s = 0$, namely $u(0) = u_T \ln(1 + 1/\varepsilon)$. Additionally, a somewhat physical interpretation is possible if one thinks of this embedding as a change $u \to su(s), u_T \to su_T$ (this highlights how the intuition driving the design of the embedding is quite different from that used for power systems). Finally, given the shape of the nonlinearity in (19), it is reasonable to expect that the analytic continuation to $s = 1$ will not encounter any singularity.

The power series coefficients for $u(s)$ are obtained in an analogous fashion to the procedures shown in Section IV. Defining the auxiliary function $E \equiv \varepsilon(e^{u(s)/u_T} - 1)$, and taking the derivative with respect to s on both sides of this definition, one obtains

$$E'(s) = \frac{1}{u_T}\left(E(s) + \varepsilon\right) u'(s).$$

Considering now the power series expansions of $E(s)$ and the derivatives $E'(s), u'(s)$, one arrives to the following relation for the coefficients at order N:

$$E[N+1] = \frac{E[0] + \varepsilon}{u_T} u[N+1] + \frac{1}{u_T} \sum_{k=0}^{N-1} \left(\frac{k+1}{N+1}\right) u[k+1] E[N-k] \tag{21}$$

Again, the embedded circuit (20) provides the other necessary relation:

$$E[N+1] = -u[N]. \tag{22}$$

For the reference germ in this case, $E[0] = 1$ and $u[0] = u_T \ln(1 + 1/\varepsilon)$. Using these starting values one can thus use recurrence relations (21) and (22) to construct the power series. Numerical experiments on this model show that the convergence properties of the resulting Padé approximant sequences are excellent, needing only about $N = 5$ power series terms in order to achieve a relative error of less than 10^{-14}. By contrast, Newton-Raphson on this simple system exhibits widely varying convergence properties depending on the choice of initial point for the iteration.

VI. Comparison With Iterative Methods

A. Conceptual Differences. Continuation Methods

In order to address a meaningful and fair comparison with iterative methods, one must first consider the conceptual differences that separate those from the holomorphic embedding method. At the core of any method based on numerical iteration we find the idea of a map that, when iterated, is expected to converge to a fixed point. One seeks maps having the *contraction* property, which in principle guarantees that the iteration will converge to a fixed point starting from any point belonging to a certain (non-empty) set. Such set is called the *basin of attraction* of said fixed point under the map. However, it is well known that these basins of attraction are hard to characterize with precision, as their borders are fractal in general. This problem is particularly relevant for power systems, where the powerflow equations contain multiple solutions, each with their own basin of attraction under the iterative scheme. Several authors have explored this fractality problem in the context of powerflow [18]–[22], showing with numerical experiments how the borders between neighboring basins intertwine in complex patterns, also interspersed with points that lead to divergence.

While it is true that in practice the basins of attraction are usually large enough to allow any experimented engineer to find a good initial point, the issue we want to stress here is that *there is no general procedure to ensure convergence to the desired solution in a completely unattended fashion, unsupervised by any human expert*. HELM was actually born out of the need

to develop new software applications for decision-support in transmission operation. There, the algorithms rely on performing a massive number of exploratory powerflows, many of them corresponding to abruptly changing scenarios. These algorithms cannot afford that a percentage of cases, however small, has a chance of diverging or mis-converging to undesired solutions. The same thing would happen to any sort of autonomous control, if it needed to rely on powerflow calculations.

Many approaches have been developed to minimize the chances of unpredictable behavior in iterative methods, but to our knowledge none of them can guarantee convergence in an automated, unsupervised fashion. This is due to the fundamental fractal behavior underlying contraction mapping-based numerical iteration. Specifically for Newton-Raphson, the Kantorovich theorem does in principle provide a criteria to find out whether a given starting point will converge or not, but this is unusable in practice because it requires computing the Lipschitz constant of the Jacobian (for a given initial guess), which is highly impractical. Moreover, if the result were negative, one would still be left with the hard problem of finding a better initial guess. Additionally, the theorem does not say anything about which solution is the desired one.

An important class of methods specifically devised to address convergence problems are those based on *homotopic continuation* [32]. These path-following methods have been used both in AC powerflows [33], [34] and for finding the DC operating point of general nonlinear circuits [13]–[15]. The apparent similarities between HELM and continuation methods warrant an extended discussion in order to clarify some important points. Like HELM, continuation methods are also based on the general idea of the embedding technique, whereby one is able to solve the problem at the "easy" limit of the embedding parameter $(\lambda = 0)$ and then follow this solution up to the value of the parameter where the original system is recovered $(\lambda = 1)$. However, the key issue is that homotopy only exploits continuity and single differentiability. It is therefore a local method, essentially. It only requires that the starting point satisfies the conditions of the Implicit Function Theorem (i.e., no degeneracy at $\lambda = 0$), and that no bifurcations are encountered on the path up to $\lambda = 1$. Certain bifurcations, namely turning points of the curve with respect to the parameter, may be overcome by switching to arc-length parameterization. In the context of finding the DC operating point of nonlinear circuits, probability-1 globally convergent continuation methods [13], [35] ensure that no bifurcations will be encountered (although there is no control as to what solution the homotopy arrives to). For these curve-tracking calculations, methods use either ODE-integration techniques or a predictor-corrector scheme, where the corrector is based on Newton-Raphson or quasi-Newton iteration. Modern continuation methods are considered to be computationally slow but robust, although their reliance on numerical iteration may still cause problems in practice [34], [36].

In contrast to homotopic continuation, the holomorphic embedding technique exploits *holomorphy*, in other words, complex analyticity. This is a much stronger condition than single differentiability. In fact, holomorphy endows the method with *global* properties, because knowledge of the power series at a given point (that is, all its derivatives) can be used to reconstruct the function everywhere, by virtue of analytic continuation. It should be emphasized that analytic continuation and homotopic continuation are two different mathematical topics that have nothing in common. Analytic continuation is a technique widely used in complex analysis to extend the domain of a given holomorphic function. In particular, for holomorphic functions given as a power series representation, it is typically used to extend the function beyond the radius of convergence of the series. For a general mathematical problem, it is not known *a priori* what analytic continuation technique can be successful (other than a cumbersome re-evaluation of the power series at a different point), or what will be the extent of the maximal domain to which the function can be analytically extended. The key point is that, in the context of the powerflow problem, the HELM method does provide a method to perform analytic continuation, and moreover, it ensures that it is maximal. This analytic continuation is provided by the sequence of near-diagonal Padé approximants constructed from the power series, as established by Stahl's theorems. As a way of showing the profound differences with homotopic continuation without delving any further in the mathematical foundations [2], a few practical differences can be pointed out: HELM is able to directly calculate the solution at *any* point along the embedded path, without needing any previous point, and the calculation is carried out by a constructive procedure in a finite number of steps.

To conclude this discussion on the conceptual differences, a few remarks must be made on a common misunderstanding about the holomorphic embedding method, regarding its use of power series and "approximants." In contrast with real analysis, where Taylor power series have limited use (they are rarely convergent, and may even converge to a value different than the function), power series play a major role in complex analysis, and even more so in the field of algebraic curves. Actually, power series are one of the major ways of *representing* holomorphic functions. Far from being an approximation, the power series *is* the function. And although the power series only converges within its radius of convergence, analytic continuation allows one to make use of the information contained in the power series to reconstruct the function well beyond that radius. Note that, for general holomorphic functions, there is no known procedure to obtain the maximal analytic continuation, but herein lies the power of Stahl's theorem: it states that, for the class of functions HELM deals with, the near-diagonal sequences of Padé approximants converge to the function in their maximal domain of analytic continuation. Therefore, the method is not limited by any convergence issues (within the limits of finite-precision arithmetic), because the successive Padé approximants can get as close as desired to the sought solution—one just needs to obtain more terms of the power series.

B. Analysis of Computational Performance

In terms of computation, the HELM method for DC systems consists of the same overall steps as for AC systems, except that most of the arithmetic operations work with real variables

instead of complex ones. The algorithmic structure of the procedure is as follows:

- Phase 1: factorize the conductance matrix.
- Phase 2: main loop:
  - Construct the members on the r.h.s. of the recurrent linear system (see (5) and (8)), using the power series terms obtained from the previous N steps.
  - Solve the linear system to obtain the power series terms at the next order, $N+1$.
  - Use these newly computed terms to calculate the value, at $s=1$, of the next Padé approximant along the stairstep of the Padé table.
  - Check for convergence by comparing the values with those obtained from previous steps; if oscillation is detected, there is no solution.

To give some idea about the number of steps typically needed in practice, it is found that around 40 to 60 terms of the power series are sufficient to achieve a numerical precision of about 10 significant digits in all but the most ill-conditioned scenarios. Ill-conditioning only happens when the system is extremely close to a branch point (this corresponds to a point of voltage collapse in power systems), but this condition is easily detectable: the number of power series terms needed to decide whether there is convergence or oscillation grows abnormally near these points. Actually, in these marginal cases there are standard techniques of power series analysis that allow predicting with precision whether the system is "just before" or "just beyond" the branching point, independently of the Padé calculations. These are seldom needed, unless one is worried about calculating the exact location of collapse points with precisions of 10 or more significant digits.

Note how, except for the overhead involved in Phase 2 steps 1 and 3, the overall computational complexity of the method is similar to fast-decoupled powerflow methods [11], [12], since the matrix is factorized only once and its factors are used repeatedly to solve linear systems (fast decoupled methods may easily take about 20 to 40 steps or more to converge, in typical applications). The admittance matrices arising from most networks are very sparse, so it is key to use a good LU sparse solver with fill-reducing permutations in order to obtain top performance. In our experience, the best results are normally obtained with the Approximate Minimum Degree fill-reducing algorithm, together with direct sparse LU solvers [37]. Note however that multifrontal and supernodal variants perform worse than the simple ones, because electric network matrices are so sparse that such blocking strategies (driven by the goal of exploiting optimized dense kernels such as the BLAS) just do not pay off.

Step 1 of Phase 2 involves the calculation of right-hand-side coefficients at order N, using all the power series terms previously calculated. This typically involves convolutions such as the ones appearing in (4), (14), (16), or (21). Thus the overall work per bus is $O(N^2)$, where N is the maximum order of the power series. Note, however, that the typical value of N is relatively low (40 to 60 maximum) and that this work is trivially parallelizable across buses.

Step 3 of Phase 2 involves the calculation of the Padé approximants for each bus voltage. As discussed in the Appendix, these are computed with algorithms whose cost is order $O(N^2)$ per bus. This cost is for the whole of Phase 2, as the construction is incremental. Just like step 1, this calculation is trivially parallelizable, as it is completely independent for each bus. Additionally, for applications where the voltage at only one bus or a few buses is needed, one may avoid the calculation of the approximants altogether, except for the designated buses. This is a very common situation in software applications that perform exploratory powerflows, for instance. Yet another performance tactic is to keep the voltage power series and only evaluate the approximants lazily, on demand.

C. Numerical Results

For the purposes of comparing HELM to existing methods, we show below the results of some numerical experiments performed using a series of medium-size network models. We have not tried to test the convergence properties of iterative methods; as discussed above, the fractal nature of the problem makes it impossible to obtain any meaningful characterization valid for general network models and scenarios, even in a statistical way. Rather, the purpose here is to provide some useful orders of magnitude about the real-world performance of HELM vs. iterative the methods, *when these converge*.

Since our current implementations do not cover yet general (i.e., non-power) DC networks of arbitrary size, the experiments have been carried out using standard IEEE test cases for AC powerflows [38]. As the reduction in computational effort resulting from going from AC to DC is expected to be similar across all methods, we believe the results will still be informative, at least for DC power systems. We have used MATPOWER [39] as a reputable implementation of the standard iterative powerflow methods, and a HELM implementation written in MATLAB, with no native code optimizations, for fair comparisons. MATPOWER also contains an implementation of the Continuation Power Flow method, which is capable of using physical parameter homotopies with arc-length and pseudo-arc-length parameterization. It does not implement probability-1 globally convergent homotopy methods, but in terms of performance most homotopy methods should be similar, as long as no bifurcations are encountered (as it is the case here).

Fig. 4 shows the results of benchmarking the CPU performance of our MATLAB-based implementation of HELM against Newton-Raphson (NR), Fast Decoupled (FD), and Continuation Power Flow (CPF) methods. The test cases were taken from the MATPOWER distribution, and range from the well-known IEEE test cases [38] to the 9200 bus test case from EU Project PEGASE [40]. When benchmarking the iterative algorithms, all cases were solved starting from the "flat start" profile (all buses set to the swing voltage), which is the best initial guess for power systems. The CPF was set up to perform an homotopy path that resembles the holomorphic embedding as much as possible, i.e., parameterizing load and generator injections as $\lambda P, \lambda Q$. MATPOWER's CPF did not allow us to interpolate the voltage of PV buses from the swing voltage to

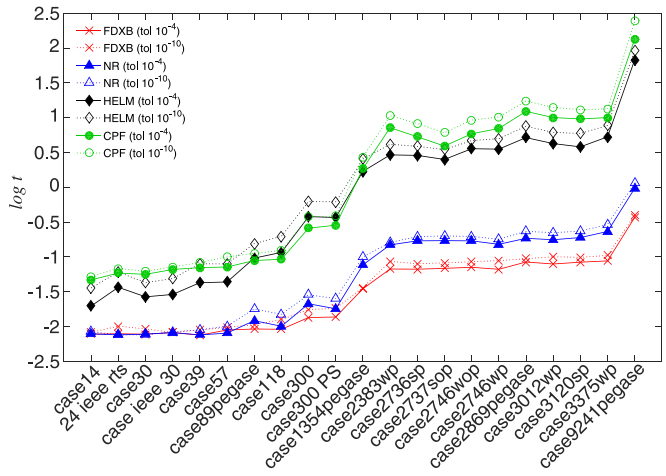

Fig. 4. CPU time benchmarks of HELMLAB (a MATLAB implementation of HELM) and various iterative algorithms in MATPOWER.

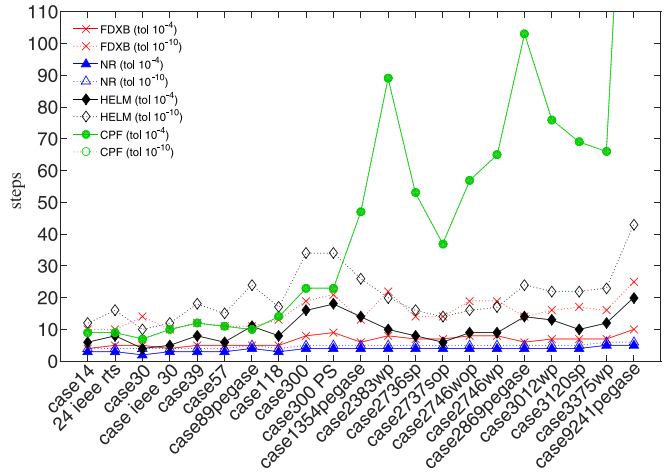

Fig. 5. Number of steps needed by each algorithm in order to attain the desired precision. Steps are iterations in the case of NR and FD, continuation steps in CPF, and order of the power series in HELM.

their respective setpoints, but this is a minor difference and it never prevented convergence. Arc-length parameterization and adaptative step-size were used.

With the exception of Gauss-Seidel, which was excluded because it failed to converge in more than half of the test cases, all algorithms were verified to converge exactly to the same solution within the required tolerance. The Fast Decoupled method was found to be the fastest in general. For clarity, only the FDXB variant shown, as the FDBX variant showed essentially the same results. The Newton-Raphson method is slightly less performant for large cases, as expected. HELM clocked at speeds about 10 to 50 times slower than NR or FD, although it should be reminded that this code had no optimizations, other than the use of the stock sparse matrix routines in MATLAB. The CPF method ran generally the slowest, even with adaptive step-size.

Nevertheless, our experience with high-performance implementations written in C has shown that the performance of HELM is actually much closer to that of NR and FD. CPU profiling indicates that the MATLAB implementation of HELM suffers from an excessive overhead in Phase 2 steps 1 and 3 (see the discussion in the preceding subsection), as these involve heavily indexed operations that MATLAB cannot vectorize and therefore are run in interpreted mode.

To complete the picture, Fig. 5 provides an idea about the number of steps that each algorithm needs to perform as the size of the model increases and as the required precision increases. NR is quite efficient in terms of the number of iterations, as one expects from its quadratic convergence rate. It achieves a tolerance of 10^{-4} in about 4–5 iterations and then it only needs one or two more to reach 10^{-10} tolerance. FD typically needs more iterations to converge, especially when more precision is required. HELM is shown to require anywhere from 10 to 20 power series terms in order to achieve a tolerance of 10^{-4}, and no more than 35 to 45 to achieve 10^{-10}. As discussed above, the only situation where more terms are needed is when the solution is very close to a point of collapse. Finally, the CPF shows a heavy increase in the number of continuation steps needed as the size of the test case grows. On the other hand, this number does not depend much on the required precision, since its predictor-corrector uses a NR method as the corrector engine.

VII. Conclusion

The Holomorphic Embedded Loadflow Method has been shown to be extensible to DC power systems. Besides constant power loads, the method can accommodate devices with general nonlinear characteristics, such as those commonly found in the onboard power distribution systems of spacecraft, aircraft, and more-electric vehicles. Additionally, the method can be extended to the wider problem of finding the DC operating points of nonlinear electronic circuits.

For power systems, the adaptation to DC has revealed that HELM's numerical properties are in general improved over its AC counterpart, even in the presence of highly nonlinear devices. On the theoretical front, DC HELM has also enabled some new exciting insights and results, some of which also benefit AC networks in return.

From the point of view of applications, the most significant advantage of the method presented here lies in its reliable and deterministic behavior. This derives from its direct and constructive nature, which completely avoids the dependency on the choice of an initial point, characteristic of methods that rely on numerical iteration. Future lines of work include exploiting this advantage in new intelligent applications for decision-support and autonomous control, for the power management systems of aircraft and spacecraft (especially unmanned autonomous vehicles), as well as autonomous DC microgrids.

On a more fundamental level, non-power DC circuits present interesting challenges to explore using this method. In particular, more work is needed on the criteria for designing the holomorphic embedding and the reference state that would yield a desired operating point. It is also worth to explore analytic continuation techniques other than Padé approximants applied to the problem of obtaining all operating points of a DC circuit.

APPENDIX
COMPUTING PADÉ APPROXIMANTS

Let $f(z)$ be a formal power series:

$$f(z) = c_0 + c_1 z + c_2 z^2 + \cdots = \sum_{N=0}^{\infty} c_N z^N. \qquad (23)$$

The *(m,n) Padé approximant* of $f(z)$ is defined as the rational function

$$[m,n]_f(z) = \frac{P_{m,n}(z)}{Q_{m,n}(z)} \equiv \frac{\sum_{j=0}^{m} p_j z^j}{\sum_{j=0}^{n} q_j z^j}$$

that satisfies

$$f(z) - [m,n]_f(z) = O(z^{m+n+1}), \qquad z \to 0. \qquad (24)$$

In other words, it is the fraction of polynomials $P_{m,n}$ and $Q_{m,n}$, of degrees at most m and n respectively, such that its Taylor power series coincides with that of $f(z)$ up to order $m+n$. The so-called *Padé table* arranges these in tabular form along m rows and n columns, which helps in revealing symmetries, recurrence formulas between their values, and many other important properties. For instance, there is an intimate relationship between certain *continued fraction* representations of $f(z)$ and the "stairstep" sequence of Padé approximants $[1,1]_f, [2,1]_f, [2,2]_f, [3,2]_f, [3,3]_f, \ldots$ Padé approximants are a powerful tool in the arsenal of numerical analysts, and have a wide array of theoretical uses in complex analysis. For general reference, see the review in [41] or the authoritative monograph [27].

In particular, if (23) is a Taylor series representing a function holomorphic in a neighborhood of $z = 0$, the Padé approximants can provide one way to obtain the analytic continuation of $f(z)$ for values of z beyond the radius of convergence of the power series. For this to work, one first needs to prove convergence of the Padé approximants to the function, which is not necessarily true in general. However, in our particular case (functions with branch points), Stahl's theorem [24] proves this convergence, and not only for a restricted region, but over the maximal domain of analytic continuation (though this only applies to near-diagonal sequences of the Padé table).

We now briefly review the landscape of numerical methods available for the calculation of Padé approximants, pointing out whether some specific issues apply or are irrelevant for the particular Padé approximants needed in HELM. The methods can divided into two large groups: on the one hand, those that compute the coefficients of $P_{m,n}$ and $Q_{m,n}$; on the other, those that directly obtain the value of the approximant at a given value (in our case, at $s = 1$). In the context of HELM, one would normally use the latter, because they are more efficient and have less chance of introducing round-off, as they involve less operations. Still, computing the polynomials might be useful for analyzing the location of singularities, for instance.

Among algorithms that compute the polynomial coefficients, [27] recommends the straightforward method—solving the associated linear system derived from (24) via LU factorization with partial pivoting—as a simple and robust strategy. This is has complexity $O(n^3)$, which could be of concern for n large, but the bigger issue here is that the Padé table can have *defects*: approximants $[m,n]_f$ for which the degree of the polynomials is less than (m,n). In such cases, the corresponding linear system is singular. More sophisticated methods, such as the Cabay-Meleshko algorithm [42], automatically overcome these problems by means of a look-ahead strategy that efficiently "jumps over" to the next normal (i.e., non-defective) approximant in the Padé table. Additionally, these methods exploit the special structure of the matrix (Toepliz); their complexity is $O(n^2)$.

Among methods that compute the value of the approximant directly, we recommend two: Wynn's epsilon and Rutishauser's quotient-difference (QD) algorithms. Both of these are $O(n^2)$, but they are based on fast recurrence relations (related to the Shanks transformation in the case of Wynn, and to continued fractions in the case of QD), so their performance is excellent in practical applications. A good description of Wynn's epsilon algorithm can be found in [43], and quality implementations appear in [44], [45]. For the QD algorithm, reference [43] contains a brief description, but the reader is advised to consult the more detailed exposition in [46] for some important implementation details.

Some careful remarks should be made about the role played by the so-called *Froissart doublets*. These are spurious pole-zero pairs appearing in the Padé approximants, having no apparent relationship to the zeros and poles of the analytic function. A formal definition of spurious poles has been given by Stahl [47], who characterizes spuriousness as an asymptotic property of the poles. Although Froissart doublets may appear from numerical round-off, particularly arising in non-normal blocks of the Padé table, they exist even in exact arithmetic. In fact, they are what prevents local uniform convergence of Padé approximants (at points other than poles or branch cuts of f) for arbitrary meromorphic functions. But for the class of holomorphic functions involved in HELM, i.e., *algebraic* functions, Stahl's theorem [24] proves convergence and therefore Froissart doublets pose no problem. Doublets induced by round-off may still appear, but they disappear or move away from the evaluation point just by increasing the Padé order. In any case, if one is interested in the detailed study of Froissart doublets, a recent method published in [48] is reported to have a remarkable ability to remove spurious doublets. The method is based on the Singular Value Decomposition, and has therefore a complexity of order $O(n^3)$.

To conclude this appendix, it is worth mentioning that there are a few "superfast" $O(n \log^2 n)$ methods based on divide-and-conquer techniques [49], but in the opinion of some authors [50] these do not have a well-established error analysis, compared to most $O(n^2)$ methods. Given the relatively low number of terms in the power series encountered with HELM in practical settings, the authors have not tried these.

REFERENCES

[1] A. Trias, "The holomorphic embedding load flow method," in *Proc. IEEE Power Energy Soc. General Meet.*, 2012, pp. 1–8.
[2] A. Trias, "Fundamentals of the holomorphic embedding load-flow method," *ArXiv e-prints*, no. 1509, p. 02421, Sep. 2015.
[3] A. Trias, "Sigma algebraic approximants as a diagnostic tool in power networks," Patent Appl. 20 140 156 094 A1, Jun. 2014.

[4] A. Gómez-Expósito and F. L. Alvarado, " Load flow," in *Electric Energy Systems: Analysis and Operation*, A. Gómez-Expósito, A. J. Conejo, and C. Cañizares, Eds., Boca Raton, FL, USA: CRC, 2009, pp. 95–126.

[5] D. Jovcic, D. Van Hertem, K. Linden, J.-P. Taisne, and W. Grieshaber, "Feasibility of DC transmission networks," in *Proc. IEEE Innov. Smart Grid Technol. (ISGT Eur.)*, 2011, pp. 1–8.

[6] A. Willson, *Nonlinear Networks: Theory and Analysis*, ser. IEEE Press Selected Reprint Series, New York: IEEE Press, 1975.

[7] L. Chua, C. Desoer, and E. Kuh, *Linear and Nonlinear Circuits*, ser. Circuits and Systems, New York: McGraw-Hill, 1987.

[8] K. J. Metcalf, "Power management and distribution (PMAD) model development: Final report," NASA Glenn Research Center, Tech. Rep. CR-2011-217268, Nov. 2011.

[9] T. Quarles, D. Pederson, R. Newton, A. Sangiovanni-Vincentelli, and C. Wayne, "SPICE, a general-purpose circuit simulation program," EECS Dept., Univ. California, Berkeley, CA, USA.

[10] W. Tinney and C. Hart, "Power flow solution by newton's method," *IEEE Trans. Power App. Syst.*, vol. PAS-86, no. 11, pp. 1449–1460, 1967.

[11] B. Stott and O. Alsac, "Fast decoupled load flow," *IEEE Trans. Power App. Syst.*, vol. PAS-93, no. 3, pp. 859–869, May 1974.

[12] R. van Amerongen, "A general-purpose version of the fast decoupled load flow," *IEEE Trans. Power Syst.*, vol. 4, no. 2, pp. 760–770, 1989.

[13] D. M. Wolf and S. R. Sanders, "Multiparameter homotopy methods for finding DC operating points of nonlinear circuits," *IEEE Trans. Circuits Syst. I, Fundam. Theory Appl.*, vol. 43, no. 10, pp. 824–838, 1996.

[14] L. Trajković, *Homotopy Methods for Computing DC Operating Points*, ser. Wiley Encyclopedia of Electrical and Electronics Engineering, Hoboken, NJ, USA: Wiley, 1999.

[15] L. Trajković, "DC operating points of transistor circuits," *IEICE Nonlinear Theory Its Appl.*, vol. 3, no. 3, pp. 287–300, 2012.

[16] D. Crutchley and M. Zwolinski *et al.*, "Globally convergent algorithms for DC operating point analysis of nonlinear circuits," *IEEE Trans. Evol. Comput.*, vol. 7, no. 1, pp. 2–10, 2003.

[17] M. H. Zaki, I. M. Mitchell, and M. R. Greenstreet, "DC operating point analysis-A formal approach," in *Proc. Formal Verification Analog Circuits (FAC)*, 2009.

[18] C. DeMarco and T. Overbye, "Low voltage power flow solutions and their role in exit time based security measures for voltage collapse," in *Proc. 27th IEEE Conf. Decision Control*, 1988, pp. 2127–2131.

[19] J. Thorp and S. Naqavi, "Load flow fractals," in *Proc. 28th IEEE Conf. Decision Control*, 1989, vol. 2, pp. 1822–1827.

[20] J. Thorp and S. Naqavi, "Load-flow fractals draw clues to erratic behaviour," *IEEE Comput. Appl. Power*, vol. 10, no. 1, pp. 59–62, Jan. 1997.

[21] R. Klump and T. Overbye, "A new method for finding low-voltage power flow solutions," in *Proc. IEEE Power Eng. Soc. Summer Meet.*, 2000, vol. 1, pp. 593–597.

[22] H. Mori, "Chaotic behavior of the newton-raphson method with the optimal multiplier for ill-conditioned power systems," in *Proc. IEEE Int. Symp. Circuits Syst. (ISCAS)*, 2000, vol. 4, pp. 237–240.

[23] H. Stahl, "On the convergence of generalized Padé approximants," *Constructive Approximation*, vol. 5, pp. 221–240, 1989.

[24] H. Stahl, "The convergence of Padé approximants to functions with branch points," *J. Approx. Theory*, vol. 91, no. 2, pp. 139–204, 1997.

[25] B. Buchberger and F. Winkler, *Gröbner Bases and Applications*, Cambridge, U.K.: Cambridge Univ. Press, 1998, vol. 251.

[26] I. Niven, "Formal power series," *Amer. Math. Monthly*, vol. 76, no. 8, pp. 871–889, 1969.

[27] G. Baker and P. Graves-Morris, *Padé approximants*, ser. Encyclopedia of Mathematics and Its Applications. Cambridge, U.K.: Cambridge Univ. Press, 1996.

[28] H. Nguyen and K. Turitsyn, "Appearance of multiple stable load flow solutions under power flow reversal conditions," in *Proc. IEEE PES General Meet. Conf. Expo.*, pp. 1–5.

[29] Y. Tamura, H. Mori, and S. Iwamoto, "Relationship between voltage instability and multiple load flow solutions in electric power systems," *IEEE Trans. Power App. Syst.*, no. PAS-5, pp. 1115–1125, 1983.

[30] B. H. Cho, J. R. Lee, and F. C. Lee, "Large-signal stability analysis of spacecraft power processing systems," *IEEE Trans. Power Electron.*, vol. 5, no. 1, pp. 110–116, 1990.

[31] Y. H. Lim and D. C. Hamill, "Nonlinear phenomena in a model spacecraft power system," in *Proc. 6th IEEE Workshop Comput. Power Electron. (COMPEL)*, 1998, pp. 169–175.

[32] E. Allgower and K. Georg, *Introduction to Numerical Continuation Methods*, ser. Classics in Applied Mathematics. Philadelphia, PA, USA: SIAM, 2003.

[33] V. Ajjarapu and C. Christy, "The continuation power flow: A tool for steady state voltage stability analysis," *IEEE Trans. Power Syst.*, vol. 7, no. 1, pp. 416–423, Feb. 1992.

[34] J. Zaborsky and M. Ilić, *Dynamics and Control of Large Electric Power Systems*, New York: Wiley-IEEE Press, 2000.

[35] R. C. Melville, L. Trajković, S.-C. Fang, and L. T. Watson, "Artificial parameter homotopy methods for the DC operating point problem," *IEEE Trans. Comput.-Aided Design Integr. Circuits Syst.*, vol. 12, no. 6, pp. 861–877, 1993.

[36] J. Roychowdhury and R. Melville, "Delivering global DC convergence for large mixed-signal circuits via homotopy/continuation methods," *IEEE Trans. Comput.-Aided Design Integr. Circuits Syst.*, vol. 25, no. 1, pp. 66–78, 2006.

[37] T. Davis, *Direct Methods for Sparse Linear Systems*, ser. Fundamentals of Algorithms, Philadelphia, PA, USA: SIAM, 2006.

[38] R. D. Christie, "Power systems test case archive," Univ. Washington, Seattle, WA, USA. [Online]. Available: https://www.ee.washington.edu/research/pstca/

[39] R. Zimmerman, C. Murillo-Sánchez, and R. Thomas, "MATPOWER: Steady-state operations, planning, analysis tools for power systems research and education," *IEEE Trans. Power Syst.*, vol. 26, no. 1, pp. 12–19, Feb. 2011.

[40] S. Fliscounakis, P. Panciatici, F. Capitanescu, and L. Wehenkel, "Contingency ranking with respect to overloads in very large power systems taking into account uncertainty, preventive, corrective actions," *IEEE Trans. Power Syst.*, vol. 28, no. 4, pp. 4909–4917, 2013.

[41] W. B. Gragg, "The Padé table and its relation to certain algorithms of numerical analysis," *SIAM Rev.*, vol. 14, no. 1, pp. 1–62, 1972.

[42] S. Cabay and R. Meleshko, "A weakly stable algorithm for Padé approximants and the inversion of Hankel matrices," *SIAM J. Matrix Anal. Appl.*, vol. 14, no. 3, pp. 735–765, 1993.

[43] A. Sidi, *Practical Extrapolation Methods: Theory and Applications*. Cambridge, U.K.: Cambridge Univ. Press, 2003.

[44] E. J. Weniger, "Nonlinear sequence transformations for the acceleration of convergence and the summation of divergent series," *Comput. Phys. Rep.*, vol. 10, no. 5, pp. 189–371, 1989.

[45] W. Press, *Numerical Recipes: The Art of Scientific Computing*, 3rd ed., Cambridge, U.K.: Cambridge Univ. Press, 2007.

[46] P. Henrici, *Applied and Computational Complex Analysis*, ser. Wiley Classics Library (Book 43), New York: Wiley-Interscience, 1993, vol. 1–3.

[47] H. Stahl, "Spurious poles in Padé approximation," *J. Comput. Appl. Math.*, vol. 99, no. 1, pp. 511–527, 1998.

[48] P. Gonnet, S. Güttel, and L. N. Trefethen, "Robust Padé approximation via SVD," *SIAM Rev.*, vol. 55, no. 1, pp. 101–117, 2013.

[49] R. P. Brent, F. G. Gustavson, and D. Y. Yun, "Fast solution of Toeplitz systems of equations and computation of Padé approximants," *J. Algorithms*, vol. 1, no. 3, pp. 259–295, 1980.

[50] B. Beckermann and G. Labahn, "Effective computation of rational approximants and interpolants," *Rel. Comput.*, vol. 6, no. 4, pp. 365–390, 2000.

Antonio Trias received the Ph.D. degree in physics from the University of Barcelona, Spain, in 1974. From 1974 to 1976 he was a Visiting Postdoctoral Research Fellow at the Lawrence Berkeley Laboratory, University of California. He is a Founding Member of Aplicaciones en Informática Avanzada S.A., where he currently is R&D Vice President and CTO. He has worked in the load flow problem and other algorithms of interest for power systems for over 20 years.

José Luis Marín received the Ph.D. degree in physics from the University of Zaragoza, Spain, in 1997. He has been a Postdoc Research Assistant at the University of Cambridge and at CEA Saclay, and a Marie Curie Research Fellow at Heriot-Watt University. In 2005 he joined Grupo AIA, where he has worked on analytic applications for power systems and other industrial problems in the utility sector. He is currently with the subsidiary Gridquant España, working on the development of HELM-based commercial tools.